Indian Journal of Chemistry
Vol. 61, December 2022, pp. 1309-1315
DOI: 10.56042/ijc.v61i12.69446

Gallic acid-cholesterol conjugate synthesis, spectroscopic characterization and quantum chemical calculations: Experimental and theoretical approach

Nadeem Ahmad Ansari, Sangeeta Srivastava* & Sadaf Aleem

Department of Chemistry, University of Lucknow, Lucknow 226 007, India

*E-mail: sangeetas.lu@gmail.com

Received 24 July 2021; accepted (revised) 17 October 2022

Gallic acid is the major constituent in fruits Phyllanthusemblica (amla), of the family phyllanthaceae. Gallic acid was first methylated to 3,4,5 trimethoxygallic acid, which upon esterification using steglich method with cholesterol resulted in the product (3S,8S,10R,13R,17R)-10,13-dimethyl-17-((R)-6-methylheptan-2-yl)-2,3,4,7,8,9,10,11,12,13,14,15,16,17-tetradecahydro-1H-cyclopenta[a]phenanthren-3-yl 3,4,5-trimethoxybenzoate. The synthesized compound has been characterized by ^{1}H NMR, ^{13}C NMR, UV, FT-IR and mass spectroscopy. Density functional theory (B3YLP) using a 6-31G (d,p) basis set has been used for quantum chemical calculations. The reactive site and reactivity within the molecule are rendered by global and local reactivity descriptors, whereas AIM (Atom in a molecule) approach illustrated weak molecular interactions within the molecule. The energies of HOMO and LUMO and frontier orbital energy gap are calculated by time dependent DFT approach using the IEFPCM model. A small value for the HOMO-LUMO energy gap indicates easier charge transfer within the synthesized compound. The nucleophilic and electrophilic reactivity is determined by MEP (molecular electrostatic potential) studies. The values calculated for polarizability, dipole moment, and first hyperpolarizability are used to depict the NLO (nonlinear optical) property of the synthesized compound.

Keywords: Steglich esterification, HOMO-LUMO, MEP, AIM, NLO

Gallic acid is an intermediary component of plant metabolism[1]. The biological efficacy of gallic acid has been described as antioxidant[2], antifungal[3], antibacterial[4], antimalarial[5], antitumor[6], anticancer[7,8], antiherpetic, antimutagenic[9], anticancer, and antiviral activities[10,11]. Synthetic gallic acid derivatives have been reported to possess number of biological and pharmacological activities. The alkyl esters of gallic acid were reported to possess anticancer, antioxidant ability and neuroprotective effect[12], scavenging free radicals[13], inducing apoptosis of cancer cells[14], inhibiting squalene epoxidase[15], interfering the signal pathways involving Ca^{2+} and oxygen free radicals[16]. The synthesized schiff bases of gallic acid were reported for analgesic, anti-inflammatory and anticonvulsant activities[17]. Gallic acid-based indanone derivatives were prepared and were found to possess anticancer activity[18].

In continuation of our work on the synthesis of conjugates of gallic acid we have synthesized (3S,8S,10R,13R,17R)-10,13-dimethyl-17-((R)-6-methylheptan-2-yl) 2,3,4,7,8,9,10,11,12,13,14,15,16,17-tetradecahydro-1H-cyclopenta[a]phenanthren-3-yl-3,4,5-trimethoxybenzoate **(3)**. Trimethoxygallic acid **(2)**[19] was derived from biologically active constituent gallic acid (**1**) isolated from Phyllanthusemblica[20]. Compound **2** was then conjugated with cholesterol yielding compound **3** using steglich method of esterification. Synthesis of compound **2** and **3** are given in Scheme 1. The structure of the synthesized compound **3** was characterized with the aid of ^{1}H, ^{13}C NMR, UV, IR techniques and mass spectrometry. Density functional theory (DFT) studies were achieved by utilizing the basis set B3LYP/6-31G(d,p) to acquire their structural properties. Same level of theory was computed for frontier molecular orbital (FMO) analysis to get inscription about their chemical reactivity and stability. Analysis of intramolecular interactions was achieved by atom in molecule (AIM) approach. Global and local reactivity descriptors gave the information about the reactive site and reactivity within the molecule. The mapping of the molecular electrostatic potential (MEP) of the stabilized molecular geometry exhibited the reactive centres. The values of dipole moment, polarizability and first hyperpolarizability of the synthesized compound **3** manifest its nonlinear optical properties.

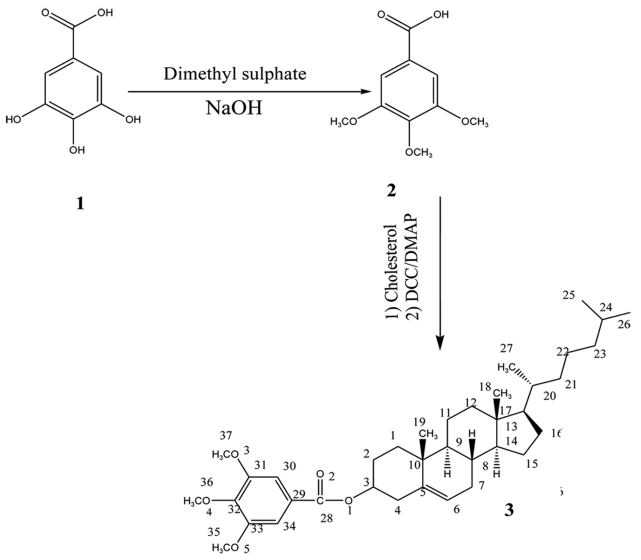

Scheme 1 — Scheme for the synthesis of compound **3**, $C_{27}H_{46}O$/DCC/DMAP, stirred at room temperature

Experimental Details

Materials and physical measurements

The reagents used for synthesis were purchased from Sigma Aldrich (St. Louis, MO). Progress of the reactions was observed through thin layer chromatography on plates coated with silica gel G coated plates. Purification of compound was made through column chromatography using silica gel (60-120 mesh). 1H NMR and 13C NMR spectra were recorded on Bruker DRX-300 MHz spectrometer and JOEL AL 300 FTNMR (75Mz), respectively, using CDCl3 as the solvent. Chemical shifts were reported as δ (ppm) using TMS as an internal reference. FT-IR spectra were recorded on Perkin Elmer FT-IR spectrometer in the range of 4000-450 cm^{-1}. ESI-MS spectrum was recorded on Agilent 6520 Q-TOF mass spectrometer. Ultraviolet absorption spectrum was obtained (in the range of 200-500 nm) using ELICO BL-200 UV-Vis spectrophotometer equipped with a 10 mm quartz cell in CHCl3 solvent for compound **3**.

Procedure for the synthesis of compound 3

90 mg (0.23 mmol) of trimethoxygallic acid and 95 mg of cholesterol was dissolved in 20 mL of chloroform and then DCC (60 mg, 0.291 mmol) and DMAP (45 mg, 0.368 mmol) were added. The reaction mixture was stirred at room temperature. The progress and the completion of reaction were monitored with the help of thin layer chromatography (TLC). Reaction mixture was first washed with 5% HCl, then by water and finally dried over anhydrous sodium sulphate and filtered. The organic layer was concentrated under reduced pressure and purified by column chromatography using ethyl acetate: hexane (20:80) yielding 80 mg of compound **3** (85.50%) as viscous white solid. Molecular formula: $C_{37}H_{56}O_5$.

Characterization of compound 3

^{1}H NMR (100 MHz, $CDCl_3$) δ (ppm): 3.91 (3H, s, OCH_3-37), 3.90 (3H, s, OCH_3-36), 3.48 (3H, s, OCH_3-35), 7.41 (1H, s, H-34), 7.41 (1H, s, H-30), 1.00 (3H, d, H-27, J=22.8 Hz), 0.92-0.91 (6H, d, H-26 & H-25, J = 3.0 Hz), 1.60 (1H, m, H-24), 1.25 (2H, m, H-23), 1.25 (2H, m, H-22), 1.21 (2H, m, H-21), 1.68 (1H, m, H-20), 1.32 (3H, s, H-19), 1.03 (3H, s, H-18), 1.45 (1H, m, H-17), 1.51 (2H, m, H-16), 1.51 (2H, m, H-15), 1.45 (1H, m, H-14), 1.57 (2H, m, H-12), 1.35 (2H, m, H-11), 1.57 (1H, m, H-9), 1.35 (1H, m, H-8), 1.95 (2H, m, H-7), 5.41 (1H, m, H-6), 2.44 (2H, d, H-4, J=7.5 Hz), 4.84 (1H, m, H-3), 1.71 (2H, m, H-2), 1.11 (2H, m, H-1).**^{13}C NMR** (75 MHz, $CDCl_3$) δ (ppm): 165.64 (C-28), 152.87 (C-33 & C-31), 142.00 (C-32), 139.63 (C-5), 125.88 (C-29), 122.84 (C-6), 106.72 (C-34 & C-30), 74.82 (C-3), 60.92 (C-36), 56.69 (C-17), 56.25 (C-14), 56.12 (C-35& C-37), 50.88 (C-9), 42.32 (C-13), 39.73 (C-12), 39.52 (C-23), 38.23 (C-4), 37.04 (C-1), 36.66 (C-20), 36.19 (C-21), 35.81 (C-10), 31.95 (C-7), 31.88 (C-8), 29.72 (C-15), 28.25 (C-2), 28.03 (C-24), 27.89 (C-16), 24.31 (C-22), 23.84 (C-25), 22.85 (C-26), 22.58 (C-11), 21.07 (C-19), 19.43 (C-18 & C-27). (ESI-MS) (Positive mode) in methanol [M+] m/z 580 (not observed), [M+1] m/z 581 (observed), IR νmax (in cm-1): 2991, 2850, 1718, 1612, 1506, 1356, 1220, 1199, 1008, 752.

Computational studies

The quantum chemical calculations on the synthesized compound was performed by DFT-B3LYP/6-31G (d,p) level of theory. To visualize the calculated data of IR and UV spectra, the GaussView 05 program was used. The time-dependent density functional theory (TD-DFT) with the same basis set with CDCl3 solvent for compound **3** executing IEFPCM model was used for electronic absorption spectra and frontier orbitals analysis of the optimized molecule. Molecular electrostatic potential surface (MEP) specifies the site of chemical reactivity of the molecule, its charge density, shape and size. Molecular interactions within the molecules were analyzed by the Atoms In Molecules (AIM) approach.

Results and Discussion

Nuclear magnetic resonance

The calculated and experimental ^{1}H and ^{13}C NMR chemical shifts (δ ppm) of compound **3** are given in Table S1 and spectra in Figs S1 and S2 in Supplementary Information**.** ^{1}H NMR spectrum of compound **3** shows the presence of singlet of two protons at δ 7.41 assigned to H-30 and H-34 and nine proton singlet at δ 3.91,3.90,3.48 for methoxy group at OCH_3-37, OCH_3-36 and OCH_3-35 suggesting the presence of trimethoxygallic acid. Signal for H-3 methine proton was obtained as multiplet at δ 4.84. Downfield shifting of H-3 methine proton indicates esterification of OH at C-3 of cholesterol. The value was comparable with the theoretical value at δ 4.29 ppm. One proton triplet was observed at δ 5.41 for H-6 methine proton of the cholesterol moiety. The downfield shifting of H-6 methine proton reveals the presence of double bond (C_5=C_6) of cholesterol, two singlet of three protons each were observed at δ 1.03 and δ 1.32 for angular methyl groups at H-18 and H-19 respectively, a characteristic of steroids. Six proton doublets at δ 0.90 confirm the presence of methyl protons for H-26 and H-25 of cholesterol. The chemical shifts observed correlates well with the theoretical values calculated in compound **3**. In ^{13}C NMR of compound **3**, signals for C-28 carbon (C=O of ester) at δ165.64 indicates ester linkage and is in good agreement with the calculated value at δ 163.13. Signals for methoxy group for C-35, C-36, C-37 in trimethoxygallic acid were observed at δ 37.04, 28.25 and 74.82 while its calculated values were found to be at δ 38.03, 35.08 and 74.42, respectively. Signals for C-30 & C-34 carbons in aromatic ring of trimethoxygallic acid moiety were notified at δ 106.72 as comparable with calculated value at δ 116.47 and 118.00 respectively. Other signals of trimethoxygallic acid were also observed and correlates well with the theoretical values. Characteristic signals for angular methyl groups at C-18 & C-19 were located at δ 19.43 and δ 21.07 respectively while its calculated values were found to beat δ 29.38 and 33.39. Signals for C-5 carbon at δ 139.63 and C-6 carbon at δ 122.84 indicate presence of a double bond between C-5 and C-6 of cholesterol moiety while its calculated values were found to be at δ 141.57 and 127.98. Other signal of the methyl groups of C-25, C-26 and C-27 of cholesterol were observed at δ 23.84, δ 22.85 and δ 19.43 respectively. Another signal at δ 74.82 assigned to carbon at C-3 shows the presence of OH group in cholesterol.

Vibrational spectral analysis

The position of carbonyl group C=O stretching vibration is determined by factors like hydrogen bonding, conjugation, ring strain and physical state. These factors give information about the environment of C=O group. In general, C=O stretching vibrations appear in the region of 1870–1540 cm^{-1}[ref.21,22]. Selected experimental and theoretical vibration wave numbers (cm^{-1}) of compound **3** are given in Table 1. In the spectrum of compound **3** given in Fig. S3, the stretching vibrations of carbonyl group (C=O) of ester at C-28 is observed at 1718 cm^{-1} while the calculated value is 1770 cm^{-1}. Stretching vibrations of C-O (C3-O1) observed at 1199 cm^{-1} whereas its theoretical value was observed at 1220 $cm^{-1}$and its reported value is 1260-1000 cm^{-1} [23]. This confirms the ester group at C-3 position. The symmetric and asymmetric C-H stretching vibration of methylene and methine proton is observed at 2991 cm^{-1} and 2850 cm^{-1} respectively whereas the calculated value is found to be at 2991 and 2791 cm^{-1}. The value is generally reported in the region 2900-3050 cm^{-1}[Ref.24,25]. The scissoring and rocking vibrations of -CH_2 are observed at 1506 and 1356 cm^{-1} and its theoretical value was found at 1507 and 1312 cm^{-1}respectively. The C=C (C31=C32) stretching vibration in aromatic ring was observed at 1612 cm^{-1}, whereas the theoretical value was found at 1608 cm^{-1} .The reported value of C=C stretching vibration within the ring in the aromatic hydrocarbon was in the region 1600 and 1585 cm^{-1} [Ref.26].

Electronic spectra and electronic transitions

The nature of the electronic transitions in the observed UV-visible spectrum of the compound **3** (Fig. S4) has been analysed by the time dependent density functional theory (TD-DFT) using B3LYP/6-

Table 1 — Experimental and selected theoretical vibration wavenumber (cm^{-1}) of compound **3**

Experimental	Calculated	Assignments
2991	2991	CH stretching in CH_2
2850	2791	CH stretching in CH
1718	1770	Ester(C=O) stretching of ester
1612	1608	C=C Stretching in aromatic ring (Trimethoxygallic acid)
1506	1507	CH_2 Bending in cholesterol
1356	1312	CH Bending in cholesterol
1220	1217	C-O bending in aromatic ring (Trimethoxygallic acid)
1199	1202	C-O stretching of ester
1008	1011	CH bending in Cholesterol
752	741	CH_2 bending in cholesterol

31(d,p) basis set. Experimental analysis of UV-visible spectrum analysis of **3** indicates one band observed at 232 nm. The experimental value 232 nm correlates with calculated value at 235 nm and is attributed to H-2→L electronic transition (n → π*) with 33.00 % contribution. The molecular orbital diagram of compound **3** is given in Fig. 1.

It reveals that the orbital HOMO-2 is localized over entire moiety of trimethoxygallic acid and the carbonyl group of the ester linkage; however orbital LUMO is localized over the ring carbons and 36-OCH_3 of trimethoxygallic acid as well as C28-O2 and C28-O1 of carbonyl group in between benzene ring and the steroidal moiety. The value of the energy gap between HOMO and LUMO is 5.60 eV. Frontier orbital energy gap helps in characterising the chemical reactivity and kinetic stability[27] of the molecule. The energies of the HOMO are associated directly to the ionization potential and therefore HOMO is preferred site for electrophilic attack. The energy of LUMO commensurate the electron affinity and therefore is preferable site for nucleophilic attack. A small frontier orbital energy gap reveals low kinetic stability, as energetically it is favourable to add electrons to a LUMO and to withdraw electrons from a HOMO. Thus, compound **3** with low frontier orbital gap is more polarizable[28] as polarizability is related with HOMO-LUMO separations. The electron dispersion can get distorted readily if the LUMO lies close to the HOMO in energy, and the polarizability is then large. If the LUMO lies high above the HOMO, an applied electric field cannot disturb the electron dispersion significantly and the polarizability is low. Therefore, soft molecules, with a small gap, will be more polarizable than hard molecules with large gap. In compound **3,** due to low HOMO-LUMO energy gap it is more polarizable and associated with high chemical reactivity which may influence the molecular activity and also displaying charge transfer interaction occurring within the molecule[29].

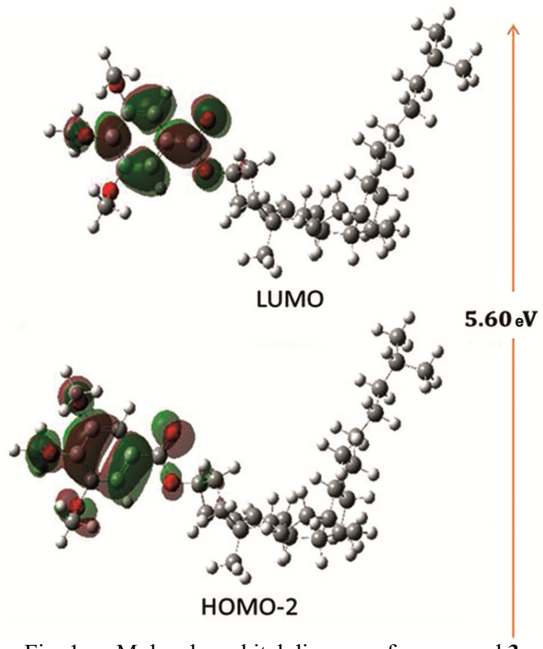

Fig. 1 — Molecular orbital diagram of compound **3**

Global reactivity descriptors

Universal postulations of chemical reactivity and molecular structural stability through the global reactivity parameters is easy to define in the light of DFT,on the basis of Koopman's theorem[30,31]. These parameters includes electrophilicity index (ω) = μ2 /2 η, electronegativity (χ) = -1/2(εLUMO +εHOMO), chemical potential (μ) = 1/2 (εLUMO + εHOMO), global hardness (η) = 1/2 (εLUMO - εHOMO) and global softness (S) = $1/2\eta$[32-35]. Larger HOMO-LUMO energy gap represents greater hardness of the molecule and direct relation to high stability and low reactivity[36]. A small HOMO-LUMO gap signifies softness and is related with more reactive molecules. Electronegativity (χ), chemical potential (μ), global hardness (η), global softness (S) and electrophilicity index (ω), the energies of frontier molecular orbitals (εHOMO, εLUMO) and frontier molecular orbitals energies gap (εHOMO- εLUMO) for compound **3** are listed in Table 2. The frontier orbital energy gap for the compound was found to be 5.2217 eV. The HOMO–LUMO energy gap of compound **3** was slightly lower, signifying lower excitation energy. Electrophilicity index decides an electrophilic or nucleophilic nature of the two reacting molecules. Higher the value of the electrophilicity index better is the electrophilic character. Owing to high values for global electrophilicity index (ω) of 2.9759 eV and chemical potential of 3.9420, compound **3** is represented as a good electrophile.

Molecular electrostatic potential

Molecular electrostatic potential surface (MESP) for the synthesized compound was obtained at DFT/B3LYP using 6-31G(d,p) basis set. MESP diagram for compound **3** and cholesterol (**CH**) is shown in Fig. 2. The significance of MESP lies in the fact that it depicts molecular size and shape as well as predicts electron density in a molecule and electronegative potential is (electron rich) region

Table 2 — Calculated εLUMO, εHOMO, energy band gap εLUMO – εHOMO, electronegativity (χ), global hardness (η), chemical potential (μ), global electrophilicity index (ω), and global softness (S) eV, using DFT/B3LYP/6-31G(d,p) level

εH	εL	εL – εH	χ	μ	η	S	(ω)
-6.5529	-1.3312	5.2217	-3.9420	+3.9420	2.6108	5.2687	2.9759

All units are in eV

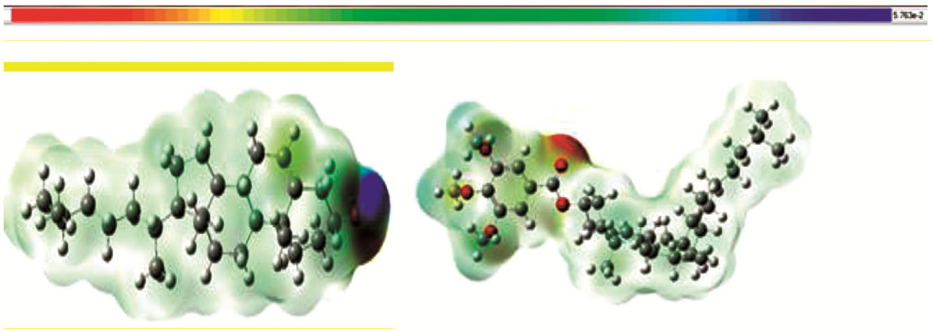

Fig. 2 — 3D plots of the molecular electrostatic potential of title compound **3**

indicated by red colour and is best suited for electrophilic attack while electropositive potential (electron poor) region is indicated by blue colour and best suited for nucleophilic attack and green region proximal to zero potential.

The electronegative potential increases (indicated by colour) in the order of red < orange < yellow < green< blue. From MESP graphics of **3** and **CH**, the H atom of the OH group of **CH** is characterized by electropositive potential (blue region) which essentially acts as an electron acceptor region suggesting comparative absence of electrons and therefore can be a site for nucleophilic attack. Thereby justifying that H atom of OH group at O1-C3 of cholesterol was esterified to the carboxylic group of trimethoxygallic acid leading to the synthesis of **3**. In compound **3,** slight electronegative region (orange region) is located over carbonyl group which essentially acts as an electron donor region and showed more magnitude of electron density, subsequently, it can be a site for electrophilic attack.

AIM calculation

Geometrical and topological parameters are convenient methods to describe the strength of hydrogen bond[37]. AIM program shows the molecular graph of compound **3** at B3LYP/6-31G(d, p) level. As reported by Rozas et al.[37], the interactions in the molecule may be classified as follows: (i) strong H-bonds are represented by $(\nabla^2\rho_{BCP}) < 0$, $H_{BCP} < 0$ and found to be covalent in nature. (ii) medium H-bonds are expressed by $(\nabla^2\rho_{BCP}) > 0$, $H_{BCP} < 0$ and found to be partially covalent in nature (iii) weak H bonds are shown by $(\nabla^2\rho_{BCP}) > 0$ and $H_{BCP} > 0$ and found electrostatic in nature. The computed electronic density (ρ), Laplacian of the electronic density ($\nabla^2\rho$), kinetic energy density (G), potential electron energy density (V) and total electron energy density (H) at the BCP (Bond Critical Point) conveys information about the nature of bonding occurring between the systems. The computational study of the QTAIM (Quantum theory of atoms in molecules) values for the bond of interacting atom is provided in Table S2. On the basis of above criteria, as $\nabla^2\rho_{BCP}$ and H_{BCP} parameters were greater than zero, hence H7.....H17, H22…..H27, H12……H17,H1…..H11, H18….H19, H35……O4, O4.....H37 are weak interactions. In this article, the Bader's theory application was used to estimate hydrogen bond energy (E). Espinosa proposed the relation between potential energy density (V_{BCP}): E = 1/2(V_{BCP}) and hydrogen bond energy (E). According to AIM calculation, the total energy of intramolecular interactions was calculated as -0.02345 kcal/mol. Molecular graph of the compound **3** using AIM program at B3LYP/6-31G(d,p) level is presented in Fig. 3.

Non-linear optical analysis

The non-linear optical properties of organic molecules have been benefited for optical switching, fibre-optic communication and optical data storage[39,40], in photonics technologies[41], in areas such as signal processing telecommunications and optical inter connections. Materials with NLO property are those in which a nonlinear polarization of light takes place during the application of an intense electric

field, when the material is exposed to a laser beam[42]. Under these conditions, the energy of the system is a function of the applied field if this electric field is homogeneous and of moderate magnitude, the system energy can be extended in the following Taylor series:

$$E = E^0 - \mu_a \Sigma E^a - 1/2\alpha_{ab}\Sigma E^a E^b - 1/6\beta_{abc}\Sigma E^a E^b E^c - 1/24\gamma_{abcd}\Sigma E^a E^b E^c E^d \quad \ldots (1)$$

where E^0 is the energy of the unperturbed molecules, E^a is the field at the origin, μ_a is component of the dipole moment and α_{ab}, β_{abc},γ_{abcd} are the polarizability, first hyperpolarizability and second hyperpolarizability tensors, respectively.

Eqn. (1) shows that polarizability and hyperpolarizability which describes the response of the system to the applied electric field. These factors govern the strength of molecular interactions as well as the NLO activities of materials. Therefore in order to investigate the molecular structure and NLO response, the first order hyperpolarizability of the novel synthesized molecular system and its corresponding (μ) and (α) are calculated using B3LYP/6-31G(d,p) level from Gaussian 09W program. The mathematical figuring of magnitude of total static dipole moment (μ_0), isotropic polarizability (α_0), and first hyperpolarizability (β_0) from entire equations using the x,y,z components is as summarized below.

$$\mu_0 = (\mu_x^2 + \mu_y^2 + \mu_z^2)^{1/2}$$

$$|\alpha_0| = 1/3(\alpha_{xx} + \alpha_{yy} + \alpha_{zz})$$

$$\mu_0 = (\mu_x^2 + \mu_y^2 + \mu_z^2)^{1/2}$$

$$|\alpha_0| = 1/3(\alpha_{xx} + \alpha_{yy} + \alpha_{zz})$$

$$\Delta\alpha = 2^{-1/2}[(\alpha_{xx} - \alpha_{yy})^2 + [(\alpha_{yy} - \alpha_{zz})^2 + (\alpha_{zz} - \alpha_{xx})^2 + 6\alpha_{xx}^2]^{1/2}$$

$$\beta_0 = [(\beta_{xxx} + \beta_{xyy} + \beta_{xzz})^2 + (\beta_{yyy} + \beta_{xxy} + \beta_{yzz})^2 + (\beta_{zzz} + \beta_{xxz} + \beta_{yyz})^2]^{1/2}$$

Since the value of the polarizability ((α_0), first hyperpolarizability (β_0) of Gaussian output are displayed in atomic unit (a.u.) and these values are altered into electrostatic unit (esu) using converting factors as (for α_0: 1 a.u. = 0.1482 x10^{-24} esu; for β_0: 1 a.u = 0.008639x10^{-30} esu). The calculated average polarizability of the molecule was 30.11x10^{-24} esu. The calculated total static dipole moment and first hyperpolarizability of 3 was found to be 2.5619 D and 24.26 x 10^{-30} esu, respectively, as shown in Table 3. Total dipole moment of molecule is approximately two times greater than that of urea and first hyperpolarizability of compound **3** is several times greater than that of urea (μ_0 and β_0 of urea are 1.3732 Debye and 0.3728 x10^{-30}esu respectively)[43,44]. Thus it is inferred that compound **3** may be an enhanced applicant in the progress of NLO materials.

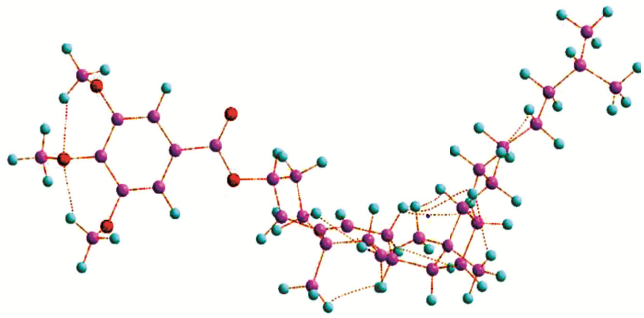

Fig. 3 — Molecular graph of compound **3** using AIM program ring critical point (red spheres) and bond path (pink lines)

Conclusion

Synthesis of compound **3**, derivative of gallic acid which was isolated from phylathusemblica, has been synthesized in high yield by Steglich method and the structure elucidation have been done. Quantum

Table 3 — Calculated Dipole moment (μ_0), Polarizability ($|\alpha_0|$) and First Hyperpolarizability (β_0) of compound **3**

Dipole moment		Hyperpolarizability	
μx	-0.9429	βxxx	538.358
μy	-0.5250	βxxy	62.4591
μz	2.3235	βxyy	-35.0914
μ_0	2.5619	βyyy	27.6168
Polarizability			
αxx	510.966	βxxz	56.1243
αyy	-0.751312	βxyz	33.7448
αzz	396.757	βyyz	2.88268
		βxzz	66.8032
		βyzz	16.0693
		βzzz	1.43370
<α>	30.11	βtotal(esu)	24.26

chemical calculations were performed with the help of density functional theory using B3LYP functional and 6-31G(d, p) basis set which correlated with the experimental results. The value for global electrophilicity index (ω) was high with 2.9759 eV which suggested it to be a good electrophile. Energy gap of 5.2217 eV indicated that easier charge transfer occurs within the molecule. As probed by AIM approach, intramolecular hydrogen bonding are found weak and electrostatic in character. On the basis of first hyperpolarizability value calculated, it is concluded that the synthesized compound **3** can be used as a good material for NLO applications and exhibit optical properties.

Supplementary Information

Supplementary information is available in the website http://nopr.niscpr.res.in/handle/123456789/58776.

Acknowledgement

The authors are thankful to the Computational section, Department of Chemistry, University of Lucknow, for providing facility for DFT and spectral analysis and to the Director, Central Drug Research Institute (CDRI), Lucknow, India for mass spectrometery measurements.

References

1 Grundhofer, Niemetz R, Schillin G & Gross G, *Phytochemistry,* 57 (2001) 915.
2 Klein E & Weber N J, *J Agric Food Chem,* 49 (2001) 1224.
3 Mahadevan A & Reddy M K, *J Plant Pathol*, 74 (1968) 87.
4 Isoyama N, Okazoe K, Ichimura N, Sugihara Y & Kono T, *NichidaiIgaku Zasshi,* 27 (1968) 270.
5 Thompson P E, Moore A M & Reinertson W J, *Antibiot. Khimioter*, 3 (1953) 399.
6 Serrano A, Palacios C, Roy G, Cespon C , Villa M L , Nocito M & Gonzales - Porque P, *Arch Biochem,* 350 (1998) 49.
7 Sharma S, Wyatt G P & Steele V E, *Methods Cell Sci,* 19 (1997) 4548.
8 Kim Y J, *Biol Pharm Bull*, 30 (2007) 1052.
9 Gentile J M, Rahimi S, Zwiesler J, Gentile G J & Ferguson L R, *Mutat Res*, 402 (1998) 289.
10 Indap M A, Radhika S, Motiwale L & Rao K V K, *Indian J Pharm Sci*, 68 (2006) 470.
11 Kratz J M, Andrighetti - Fröhner C R & Leal P C, *Biol Pharm Bull*, 31 (2008) 903.
12 Locatelli C, Filippin M F B & Creczynski P T B , *Eur J Med Chem*, 60 (2013) 233.
13 Dwibedy P, Dey G R, Naik D B, Kishore K & Moorthy P N, *J Phys Chem A,* 1 (1999) 1915.
14 Saeki K, You A, Isemura M, Abe I, Seki T & Noguchi H, *Biol Pharm Bull*, 23 (2000) 1391.
15 Abe I, Seki T & Noguchi H, *BiochemBiophys Res Commun*, 270 (2000) 137.
16 Sakaguchi N, Inoue M & Ogihara Y, *Biochem Pharmacol*, 55 (1998) 1973.
17 Kumara Prasad S A, Subrahmanyam E V S & Shabaraya A, *World J Pharm Res,* 3 (2014) 2741.
18 Saxena H O, Faridi U, Srivastava S, Kumar J K, Darokar M P, Luqman S, Chanotiya C S, Krishna V, Negi A S & Khanuja S P S, *Bioorg Med Chem Lett* 18 (2008) 3914.
19 Srivastava S, Ansari & A N, Aleem S, *Lett Org Chem,* 18 (2021) 134.
20 Srivastava S, Ansari N A & Aleem S, *J Biol Chem Research*, 36 (2019) 14.
21 Silverstein R M & Webster F X, *Spectrometric Identification of Organic Compounds*, sixth ed., (Jon Wiley Sons Inc, New York) 1963.
22 Singh R P, Kant R, Singh K, Sharma S & Sethi A, *J Mol Struct*, 109 (2015) 125.
23 Lin-Vien D, Colthup N B, Fateley W G & Grasselli J G, *The Handbook of Infrared and Raman Characteristic Frequencies of Organic Molecules*, (Academic Press, New York) 1991.
24 Roeges N P G, *A Guide to the Complete Interpretation of Infrared Spectral of Organic Structures*, (John Wiley and Sons Inc, New York) 1994.
25 Colthup N B, Daly L H & Wiberly S E, *Introduction to Infrared and Raman Spectroscopy*, (Academic Press, New York) 1975.
26 Krishnakumar V, Manohar S & Nagalakshmi R*, Spectrochim Acta Part A*, 71 (2008) 110.
27 Aihara J, *J Phys Chem A,* 103 (1993) 7487.
28 Bhavani K, Renuga S, Muthu S & Sankaranarayanan K, *Spectrochim Acta Part A,* 136 (2015) 1260.
29 Luo J, Xue Z Q, Liu W M, Wu J L & Yang Z Q, *J Phys Chem A,* 110 (2006) 12005.
30 Fukui K, *Science*, 218 (1982) 747.
31 Pearson R G, *J Org Chem*, 54 (1989) 1423.
32 Pearson R G, *Chemical Hardness Applications from Molecules to Solids*, (VCH Wiley Weinheim) 1997.
33 Yang W & Parr R G, *Proc Natl Acad Sci,* 82 (1985) 6723.
34 Parr R G & Szentpaly L V S, *J Am Chem Soc*, 121 (1999) 1922.
35 Machura B, Wolff M, Palion J & Kruszynski R, *Inorg Chem Commun*, 14 (2011) 1358.
36 Nowrooi A & Raissi H, *J Mol Struct*, 759 (2006) 93.
37 Rozas I, Alkorta I & Elguero J, *J Am Chem Soc,* 122 (2000) 11154.
38 Powell C E, Morrall J P, Ward S A, Cifuentes M P, Motaras E G A, Samoc M & Humphrey M G, *J Am Chem Soc,* 126 (2004) 12234.
39 Zhou X, Feng J K & Ren A M, *Chem Phys Lett*, 403 (2005) 7.
40 Yunus K, Yilmaz V T & Buyukgungor O, *Molecules*, 21 (2016) 1.
41 Arivuoli D, *Pramana - Journal of Physics,* 57 *(*2001) 871.
42 Patel N B & Patel J C, *Arab J Chem,* 4 (2011) 403.
43 Zayed M F & Hassan M H, *Saudi Pharmaceut J*, 22 (2014) 157.
44 Khattab S N, Haiba N S, Asal A M, Bekhit, A A, Guemei A, Amer A & El-Faha A*, Bioorg. Med Chem Lett*, 27 (2017) 918.